
Wing angle
90°
Wing angle
110°
Forced flight
0
1
2
3
4
5
6
7

The Journal of Experimental Biology 204, 2209–2220 (2001)
Printed in Great Britain © The Company of Biologists Limited 2001
JEB3308

FLIGHT-MOTOR-DRIVEN RESPIRATORY AIR FLOW IN THE HAWKMOTH *MANDUCA SEXTA*

LUTZ T. WASSERTHAL*

Institut für Zoologie I, Universität Erlangen-Nürnberg, Staudtstrasse 5, D-91058 Erlangen, Germany

*e-mail: ltwthal@biologie.uni-erlangen.de

Accepted 3 April 2001

Summary

Intratracheal pressure during tethered flight was analyzed at the anterior spiracles and mesoscutellar air sacs in the hawkmoth *Manduca sexta* using electronic pressure sensors. CO_2 emission from the anterior spiracles and the posterior thoracic and abdominal spiracles was measured using a URAS gas analyzer with a split-specimen chamber. Experiments were accompanied by photocell recordings of the wingbeat. The structural differences between the mesothoracic and metathoracic spiracles are described. Deformations of the lateral thorax and their effect upon the spiracles were observed under stroboscopic light.

During shivering, ventilation pulses are generated by the flight muscles reminiscent of an autoventilation mechanism with tidal air flow. During steady flight, however, a unidirectional airstream arises with a mean negative (subatmospheric) pressure at the first (mesothoracic) spiracles and a mean positive pressure in the mesoscutellar air sacs. As a result of this pressure difference during flight, CO_2 is emitted only at the posterior spiracles.

The suction force for the inspiration flow at the anterior spiracles is generated by the flight apparatus as a result of prevention of inspiration through the posterior thoracic spiracles. During the downstroke, the volume of the thoracic air sacs increases, while the posterior thoracic spiracles are automatically enclosed in the subalar cleft below the wing hinge and are probably closed. During the upstroke, the air sac volume decreases and the moth expires through the open posterior spiracles.

Key words: insect, respiration, air pressure, CO_2 emission, trachea, spiracle, flight, muscle, gas supply, hawkmoth, ventilation, Sphingidae, *Manduca sexta*.

Introduction

Investigations of insect respiration using modern sensors and recording techniques have been performed predominantly in resting insects and in developing instars (Gunlinson and Harrison, 1997; Hadley, 1994; Harrison, 1997; Hetz et al., 1993; Hetz et al., 1999; Kestler, 1984; Lighton, 1996; Slama, 1976, 1988; Wasserthal, 1976; Wasserthal, 1981; Wasserthal, 1982; Wasserthal, 1996; Wasserthal, 1999). Although flying is one of the most fundamental characteristics of higher insects, only relatively little experimental work has focused on the supply mechanism for the flight motor in insects. Because of methodological difficulties, measurements of intact unnarcotized insects during activity, especially during flight, are almost lacking.

In insects such as locusts, hymenopterans, scarabaeid beetles and hawkmoths, the abdominal pumping movements observed during flight are assumed to contribute to respiratory gas exchange in the flight muscles (Snodgrass, 1935; Fraenkel, 1932a), but the effects of this abdominal pumping on tracheal ventilation of the thorax have rarely been measured. Our knowledge regarding respiration during insect flight is based mainly on the work of P. L. Miller (Miller, 1960; Miller, 1966; Miller, 1974; Miller, 1981) and Weis-Fogh (Weis-Fogh, 1964a; Weis-Fogh, 1964b; Weis-Fogh, 1967).

In locusts, haemolymph pressure data gave rise to the autoventilation model (Weis Fogh, 1964a; Weis-Fogh, 1967). Air is assumed to be sucked in and blown out equally through all the thoracic spiracles by deformations of the air sacs around and between the flight muscles as a consequence of wing movements. In locusts, a unidirectional flow between the anterior body and the abdomen caused by abdominal pumping was measured that contributed to the tidal flow of autoventilation (Miller, 1960; Weis Fogh, 1964a; Weis-Fogh, 1967).

In flying cerambycid beetles, the volume of air passively entering the exposed anterior spiracles and passing through the primary tracheae was analyzed and termed ‘through-draught ventilation’ (Miller, 1966). In these beetles, this mechanism is assumed to be combined with autoventilation of the smaller secondary tracheae.

As powerful fliers, hawkmoths are capable of increasing their metabolic rate by up to 148-fold from rest to full flight (Bartholomew and Casey, 1978). They therefore have, like hummingbirds (Berger and Hart, 1972), one of the highest

recorded metabolic rates. It is unclear how hawkmoths manage to meet the increased O_2 demands during flight with their tracheal supply system, and the mechanism of air flow remains unresolved. Remarkably, the O_2 content of the flight muscles during steady flight exceeds even the resting level (Komai, 1998). It is the aim of the present study to contribute to the understanding of this very efficient supply mechanism. Special care was taken to use healthy moths and to avoid invasive techniques and unphysiological conditions as far as possible.

Materials and methods

Animals and handling procedures

Since commercially obtainable *Manduca sexta* often show genetic deficiencies as a result of inbreeding, I used offspring derived from a laboratory stock from the Department of Animal Physiology, Marburg, Germany, that has been 'replenished' with stocks from Seattle and Cologne. Only individuals that were relatively long-lived and strong flyers were used in experiments. The adults were kept in a flight room prior to the experiments and were allowed to feed from artificial flowers containing a 15 % honey solution. For experiments, 5- to 10-day-old healthy moths (N=6; body mass range 1.4–2.6 g) were selected.

Moths were suspended at the descaled mesoscutellum with elastic layers of 'Pattex' (Henkel, Düsseldorf, Germany) from a rigid rod. Narcosis was avoided throughout all procedures. Instead, preparatory steps were carried out very gently, allowing recovery periods of several hours. To stimulate flight, the normal nocturnal activity rhythm was used; dimming of the room light was sufficient. The moths frequently flew for several hours without further encouragement, such as using a fan. The moths remained suspended for the entire experimental period over 3–5 days. They were fed *ad libitum* with a 12–18 % honey solution at the beginning and sometimes again at the end of the recording session, which lasted several hours. At the end of the experiments, the moths were still healthy and could be separated from the mounting rod. All moths were used first for tracheal pressure measurements and then for CO_2 emission measurements. The experiments were performed in a Faraday cage at 20±1 °C.

The wingbeat was recorded by projecting the shadow of the left or right or both moving wings onto one or two silicon photocells (Conrad 55 mm×20 mm or Telefunken BPY 10 mm×3 mm) installed on the bottom of the Perspex specimen chamber. For high-resolution analysis of wing position in relation to the course of a tracheal pressure pulse, the shadows produced by the wing were projected on two vertically arranged sensors. One sensor was shaded by the wing during upstroke, the other one was shaded during downstroke. Both sensors show the complete wingbeat cycle, but the arrangement was optimal when the curves of both sensors were symmetrical. Only the curve of the sensor shaded during the downstroke was used for the documentation of wing movement (see Fig. 6). For this high temporal resolution, the sampling rate was increased to 40 kHz; in contrast, 400 Hz was used during most long-term measurements. The photocell voltage signal showed a delay of 2.5–3 ms relative to the pressure pulse which was accounted for in the analysis of the recordings (e.g. in Fig. 6). For observations of thoracic deformation and

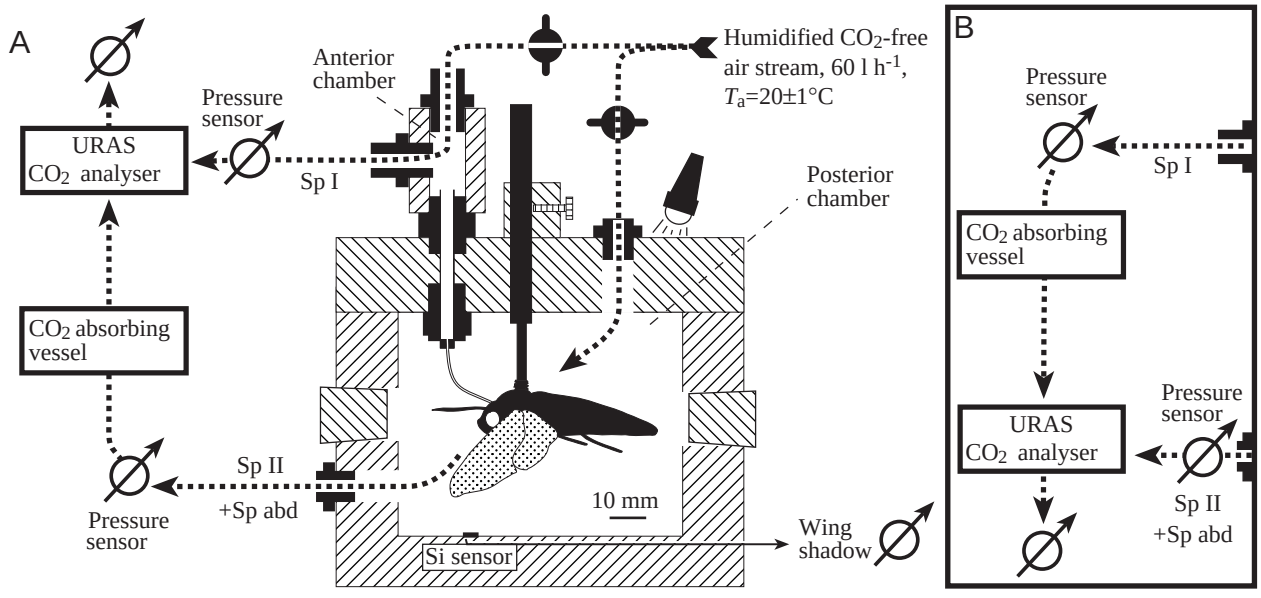

Fig. 1. Split-specimen chamber used for measuring CO_2 emission from specified spiracles of hawkmoths. The device allows the air pressure in both chambers to be measured and adjusted. In A, the anterior chamber with the air flow from the anterior spiracles is connected to the CO_2 analyser directly, and the posterior chamber with the air flow from all other spiracles is connected to the CO_2-absorbing vessel. In B, the air flow passing through the posterior chamber is conveyed directly to the CO_2 analyser, while the air flow from the anterior chamber passes *via* the CO_2-absorbing vessel. The wingbeat is recorded by projecting the shadow of the wings onto a silicon photocell installed on the bottom of the transparent experimental chamber. Sp I, mesothoracic spiracle; Sp II, metathoracic spiracle; Sp abd, abdominal spiracles.

spiracular activity, the left side of the thorax was descaled and illuminated using an industrial strobelight (Drello, Mönchen Gladbach, Germany).

Tracheal pressure measurements

The cuticle around both first (=anterior=mesothoracic=Sp I) spiracles was carefully descaled, and polyethylene tubes (1 mm external and 0.5 mm internal diameter) were tightly glued using 'Fixogum' rubber cement (Marabu, Tamm, Germany) around the perimeter of the intact spiracle. The tube from each side could be connected independently directly to a pressure sensor (Sensym SCXL 004 DN) or both tubes could be connected to the smaller compartment of a split-specimen chamber and their outputs combined for either pressure or CO_2 emission measurements (Fig. 1). Blocking both anterior spiracles with pressure sensors at the same time induced intermittent flight, probably as a result of anoxia (see Fig. 5A). Long-term pressure measurements were therefore conducted with only one of the anterior spiracles connected to the pressure sensor or with the sensors intermittently disconnected. Optimal flight temperature was assumed to be attained in the experiments after the transition from shivering to full flight; in a recent study using *Agrius cingulatus* and *Hippotion celerio*, contact thermometric measurements at the aorta have shown optimal flight temperature to be reached after 3–4 min of shivering and to be maintained during typical flight phases of 3–6 min, even when they were interrupted by short pauses (L. T. Wasserthal, in preparation).

As the second (posterior thoracic=metathoracic=Sp II) spiracles are integrated into the wing hinge and are not accessible during flight, it was impossible to fix tubes to these spiracles. The intratracheal pressure in the posterior thorax was therefore measured at the mesoscutellar air sac on the rear of the mesotergal pulsatile organ (PO II) on top of the dorsal longitudinal muscles (DLMs) (Fig. 2). For this purpose, an 'artificial spiracle' was created by puncturing the cuticle and the underlying air sac. A polyethylene tube was connected to the hole in the air sac and fixed to the mounting rod to prevent positional changes of the tube with respect to the air sac that could cause artificial pressure pulses. The electronic pressure data were calibrated using a mechanical barometer (2500 Pa total scale). The low-pass filter effect of the pressure sensors with increasing pulse frequencies was analyzed using a woofer-loudspeaker that broadcast certain frequencies inside the specimen chamber calibrated with a Bruel & Kjaer 0.5 inch microphone to a 2331 sound level meter. The amplitude correction factor for two sensors was 1.37 and 1.86, respectively, at a pressure pulse frequency of 26 Hz. Scales in the figures represent the corrected pressure amplitudes.

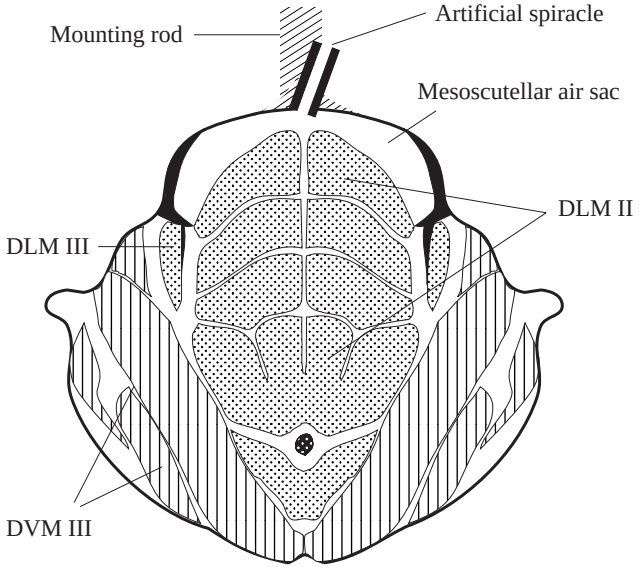

Fig. 2. Semi-schematic cross section of the region between the posterior mesothorax and anterior metathorax at the level of the mesoscutellar air sac showing the positions of the mounting rod and artificial spiracle (based on X-ray tomography and histological sections). DLM II, DLM III, dorsolongitudinal muscles of the mesothorax and metathorax, respectively; DVM III, dorsoventral muscle of the metathorax.

CO_2 measurements

CO_2 measurements were performed in a split-specimen chamber with a controlled constant-speed air flow ($60\,l\,h^{-1}$) and adjustable pressure at a temperature of 20±1 °C (Fig. 1). For smaller individuals (mass 1.4 and 1.6 g, N=2), a specimen chamber with a working volume of 83 mm×94 mm×62 mm was used. For larger moths (mass 1.9–2.6 g, N=4), a cylindrical specimen chamber with an inner diameter of 112 mm and a height of 65 mm was used. To obtain the best possible CO_2 measurements, it was important to keep the chamber volume as small as possible. Care was taken that the movements of the wings were not restricted by the chamber wall or by the mounting rod or attached sensors. Flight was initiated some hours after the moths had been mounted in the chamber. Lateral openings in the chamber allowed the moth to be fed and the tissue patch provided for foot contact to be manipulated to quieten the moth at the end of a flight session. The tubes leading from the anterior spiracles (Sp I) were connected to the small anterior compartment of the split-specimen chamber. The posterior thoracic (Sp II) and abdominal (Sp abd) spiracles opened into the larger posterior specimen compartment.

For CO_2 measurement, the air flow from either the anterior (Fig. 1A) or the posterior compartment (Fig. 1B) was conveyed directly to an infrared gas analyzer URAS 3G (Hartmann & Brown) while the air from the other compartment was conveyed to a CO_2-absorbing vessel containing NaOH. The pressure within both compartments was normally adjusted to the same value (between 10 and 100 Pa). The detection limit was approximately $0.05\,\mu l\,s^{-1}$ in the smaller specimen chamber and $0.1\,\mu l\,s^{-1}$ in the larger one; the response time of the system was 1.4±0.2 s. The baseline of the CO_2 analyser and system was checked for drift after each experiment without the moth. In some experiments, the pressure of the posterior chamber was slightly increased to avoid an artificially high pressure at

the anterior spiracles that would have prevented CO_2 emission at Sp I and, thus, might have caused unnaturally high CO_2 outputs at Sp II. A higher pressure in the posterior chamber should produce increased outflow through the anterior spiracles. The CO_2 output was calibrated for each pressure regime and specimen chamber after the experiments using a motor-driven 50 ml syringe simulating the release of a constant volume of pure CO_2 at different rates (0.1–20 µl s^{-1}). Data were acquired using an eight-channel MacLab interface, and calculations were performed using Chart 3.63 software on Power Macintosh computers.

Spiracle morphology

After descaling and cleaning, the thoracic spiracles were examined using a binocular microscope and photographed using a custom-made light scanning microscope and a field-emission scanning microscope at 2 kV accelerating voltage (Hitachi S 800). For scanning electron microscopy, specimens were air-dried, gold-coated for 3 min under argon plasma at 25 mA and 2 kV (Hummer JR) and glued with colloidal silver to aluminium stubs.

Results

Intratracheal pressure

In the hawkmoth *Manduca sexta*, intratracheal pressure pulses at the anterior spiracles and mesoscutellar air sac are synchronous with the wingbeat (see Fig. 4, Fig. 6). Mean frequency is 27±3 Hz (mean ± S.E.M., N=6). During shivering, the mean pressure oscillates around ambient with an amplitude ranging between approximately 20 and 100 Pa (Fig. 3A). During steady flight, the pressure amplitude increases in conjunction with the increased wingbeat amplitude to between 50 and 250 Pa at the anterior spiracles (Sp I) and between 100 and 450 Pa at the mesoscutellar air sac (Fig. 3B, see Fig. 6).

At the anterior thoracic spiracles, the mean pressure is between −10 and −70 Pa (Fig. 3, Fig. 4, Fig. 5A, Fig. 6). In contrast, in the mesoscutellar air sac during steady flight, the mean pressure is between +20 and +50 Pa above atmospheric pressure (Fig. 3, Fig. 4, Fig. 5B, Fig. 6). The resulting pressure gradient ΔP between the anterior spiracles and the posterior dorsal air sacs is 30–120 Pa. This suggests that inspiration of fresh air at the anterior spiracles and expiration at the posterior spiracles will occur.

A single wingstroke in *Manduca sexta* lasts between 32 and 41 ms. Analysis of pressure changes during a single wing stroke showed that the intratracheal pressure minimum at both measuring sites coincided with the second half of the downstroke (Fig. 6). The pressure maximum occurred during the last third of the upstroke. The maximum and minimum pressures at Sp I and the mesoscutellar air sac often coincide but may also be slightly shifted in time, with the maximum at the mesoscutellar air sac occurring 1.2–2.5 ms earlier than that at Sp I. The pressure minima of the mesoscutellar air sac and anterior spiracles could be shifted in both directions by 0.8–1.3 ms.

CO_2 emission

To investigate whether the observed pressure difference between Sp I and the mesoscutellar air sac affects the pattern of air flow in the thorax, CO_2 measurements in the split-specimen chamber were performed with the same air flow speed and pressure in both chambers. No CO_2 emission was recorded from the anterior spiracles, which opened into the anterior chamber (Fig. 1A, Fig. 7A). All recorded CO_2 emission was from the posterior spiracles (Fig. 1B, Fig. 7B). Even when the pressure in the posterior chamber was higher (ΔP up to 25 Pa) than in the anterior chamber, the CO_2-containing air stream was not reversed (Fig. 8, Fig. 9). Only when the pressure in the posterior chamber was artificially raised to more than 25 Pa above that of the anterior chamber was CO_2 expired at the anterior spiracles. The moths were only capable of short periods of flight under these imposed pressure differences (Fig. 9). Under these conditions, CO_2 emission increased at the anterior spiracles during pauses between flights and decreased again during flight periods with a latency of 1–1.5 s. A complete reversal of CO_2 output from the anterior spiracles could not be achieved by the application of a higher pressure to the posterior chamber.

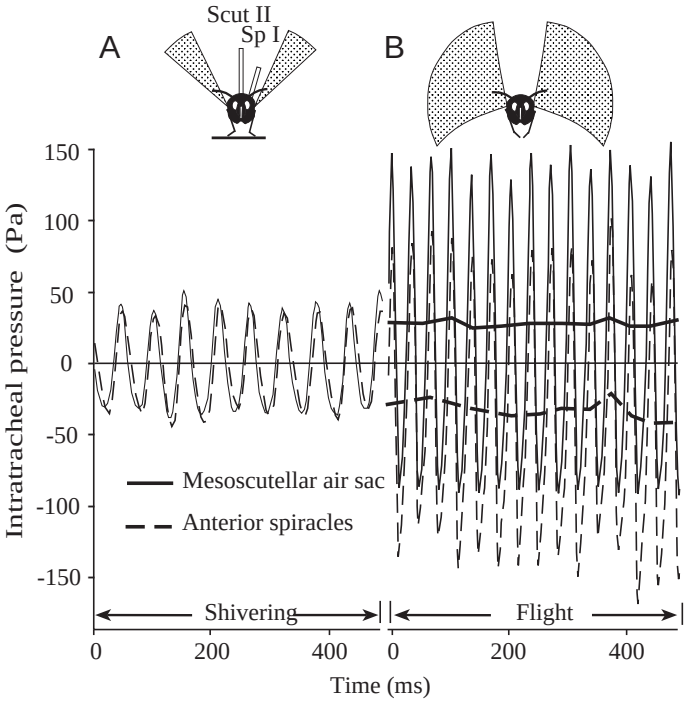

Fig. 3. Intratracheal pressure relative to atmospheric pressure during shivering (A) and steady flight (B) in tethered *Manduca sexta*. During shivering, the mean pressure is approximately equal to atmospheric pressure (0 Pa on this scale). During flight, the mean pressure at the anterior spiracles (Sp I, horizontal broken line) is negative, whereas that at the mesoscutellar air sac (Scut II, horizontal thick line) is positive. The inset moth pictures show wing position and wingbeat amplitude. Sampling rate was 40 kHz.

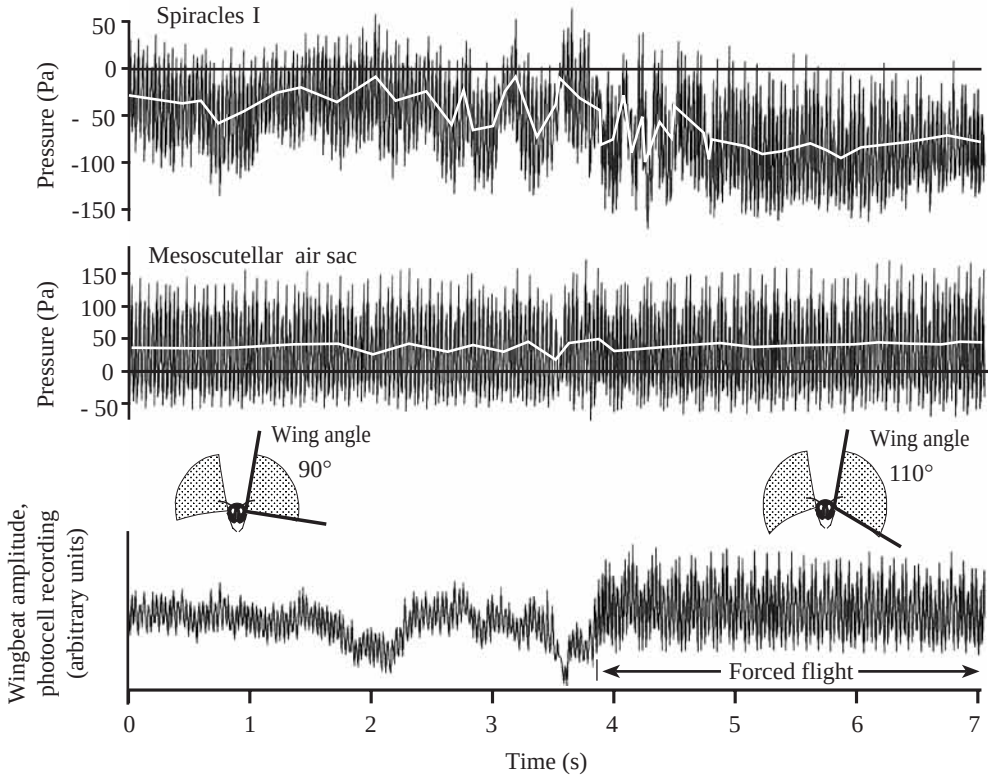

Fig. 4. Intratracheal pressure measured at the anterior spiracles (spiracles I) and mesoscutellar air sac during steady flight in *Manduca sexta* and with increased wingbeat amplitude during forced flight. At the anterior spiracles, the mean pressure is negative, and pressure pulse amplitude increases with wingbeat amplitude, with mean pressure (white line) becoming more negative. At the mesoscutellar air sac, the mean pressure (white line) is positive and is less affected by the increased wingbeat amplitude. Wingbeat amplitude was measured as the amount of shade cast by the moving wing onto a laterally arranged silicon photocell. Maximum values of shading curves (the lowest voltage produced by the photocell) correspond to highest amplitudes. Sampling rate was 40 kHz.

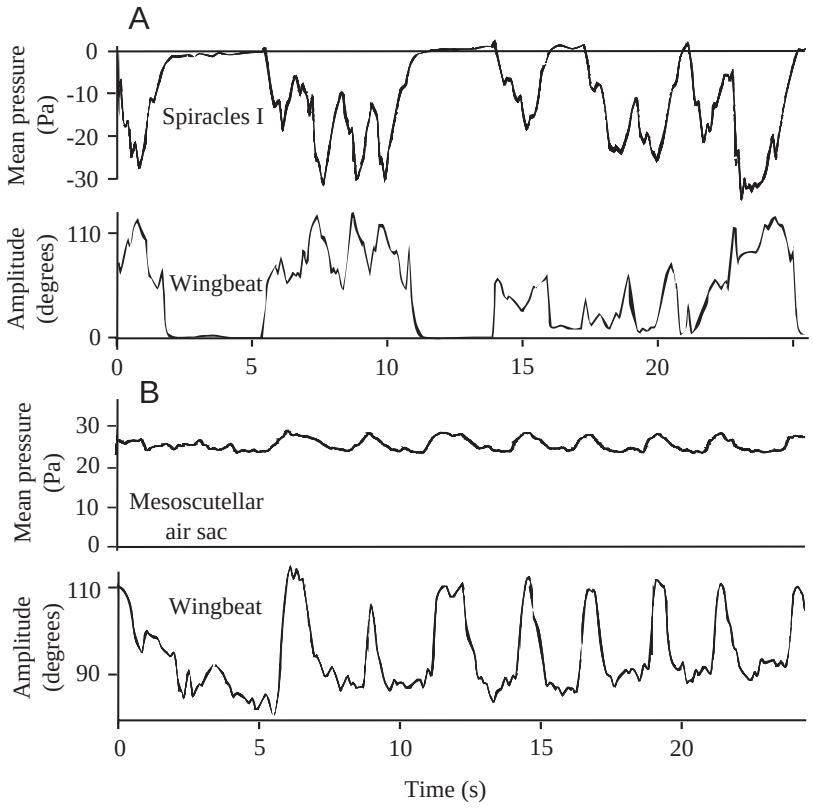

Fig. 5. Effects of wingbeat amplitude on mean intratracheal pressure during flight in *Manduca sexta*. (A) At the anterior spiracles (spiracles I), the wingbeat amplitude maxima coincide with the pressure minima. (B) At the mesoscutellar air sac, the wingbeat amplitude maxima coincide with the pressure maxima. Recording techniques are as described in the legend to Fig. 4. Voltage values for wingbeat curves have been converted into angular degrees of wing position from 0° (no flight) to 110° (with maximum angle corresponding to maximum wing-stroke amplitude during steady flight).

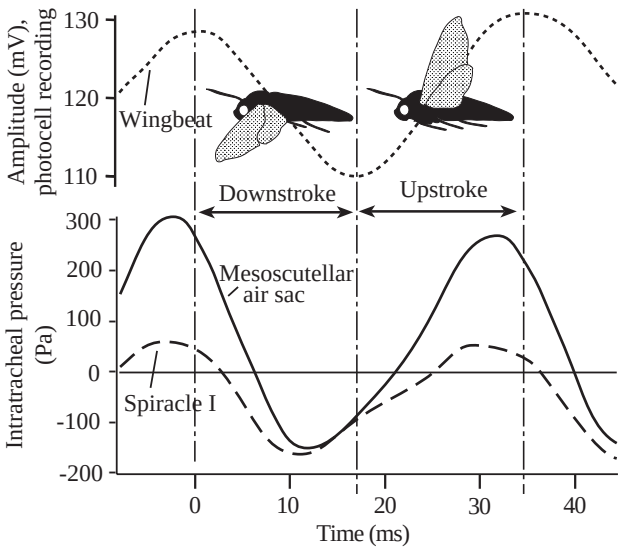

Fig. 6. Intratracheal pressure changes measured at the anterior spiracle (spiracle I) and at the mesoscutellar air sac during a single wingbeat in *Manduca sexta*. Recording techniques are as described in the legend to Fig. 4. The pressure minima occur during the downstroke (110 mV), the maxima during the upstroke (128 mV).

Functional characterisation of the thoracic spiracles

The anterior spiracle (Sp I), the mesothoracic spiracle, is situated in the flexible intersegmental membrane between the prothorax and mesothorax. It is hidden under scales and its orifice is protected from dust or particles by a pair of peritrema lamellae (Fig. 10A). Each lamella consists of approximately six rows of cuticular processes connected by anastomoses, thus forming a three-dimensional meshwork (Fig. 10C,D). The position of this spiracle is not significantly affected by the wingstroke. Closing and opening of the inner valve can be observed only after removal of the two peritremal filter lamellae (Fig. 10B). The pressure curves (e.g. Fig. 3) suggest that these valves are held open during steady flight. Changes in amplitude of the pressure signal are correlated with changes in wingbeat amplitude (Fig. 5A), with no superimposed effect of valve opening or closing observed.

The posterior thoracic spiracle (Sp II) has no peritrema filter apparatus, instead having a single external valve flap at the anterior side of the orifice and spinose perispiracular cuticle (Fig. 11). This valve is assumed to be closed by a ventral muscle and opened as a result of cuticle elasticity (Nüesch, 1953; Eaton, 1988; Nikam and Khole, 1989). However, it has been overlooked that the functioning of this spiracle is affected by wing movements. It is located deep within the subalar

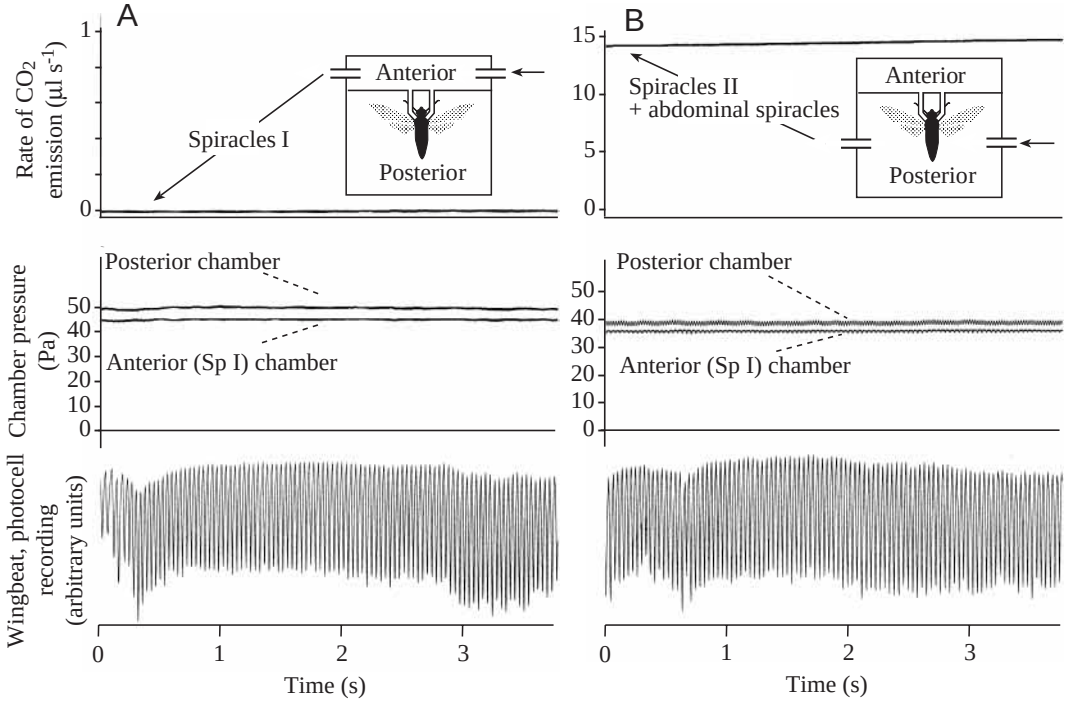

Fig. 7. CO_2 emission during steady flight in a male *Manduca sexta* (mass 1.5 g, 9 days old). The results are from a split-specimen chamber (see insets at the top of the figure). In A, only air from the anterior chamber (connected to the anterior spiracles) was conveyed to the CO_2 analyser directly, while air from the posterior chamber first passed through a vessel containing NaOH to absorb CO_2. No CO_2 emission was detected from the anterior spiracles (spiracles I), although the air presssure in the anterior chamber was slightly lower than in the posterior chamber. In B, only the air flow from the posterior chamber (including the posterior thoracic, spiracles II, and all abdominal spiracles) was conveyed to the CO_2 analyser without first passing through the NaOH vessel. All CO_2 is expired from these posterior spiracles. Sampling rate was 400 Hz.

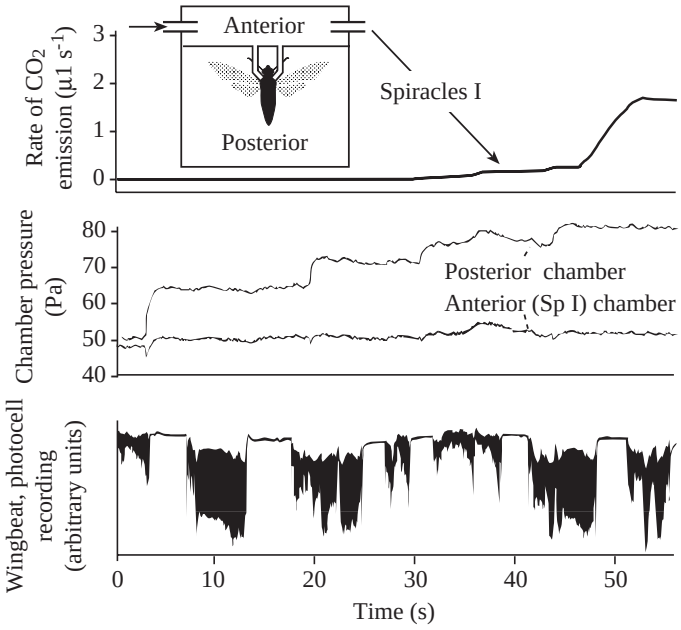

Fig. 8. Induced respiratory flow reversal causing CO_2 emission from the anterior spiracles (spiracles I) during flight of a male *Manduca sexta* (mass 1.4 g, 10 days old). Results from a split-chamber experiment (see inset at the top of the figure) with stepwise pressure increases applied to the posterior chamber. CO_2 emission from the anterior spiracles (Sp I) begins when the pressure difference ΔP between the posterior chamber and the anterior chamber exceeds 25 Pa. Sampling rate was 400 Hz.

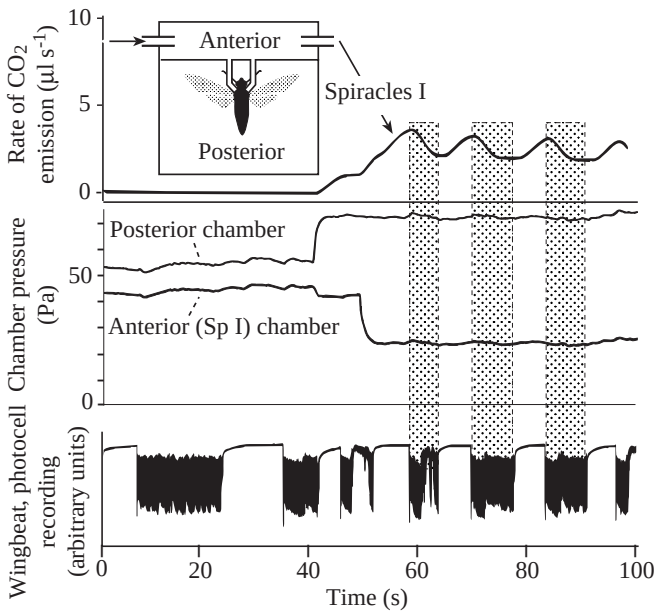

Fig. 9. Effects of intermittent flight activity on CO_2 emission from the anterior spiracles (spiracles I) in a split-chamber experiment. Application of an artificial pressure difference ΔP of approximately 50 Pa between the two chambers produced a CO_2 output from the anterior spiracles (Sp I) of approximately 2.5 µl s^{-1}. During the pauses between flights, CO_2 output rises to approximately 3.5 µl s^{-1}; it then decreases again during the flight phases (stippled) with a latency of approximately 1 s. Sampling rate was 400 Hz.

intersegmental cleft, which is subjected to positional changes during flight. These movements and their influence upon Sp II were observed under stroboscopic light and viewed from slightly below. The wing movements of the flying moth were 'frozen' by interference between the flash rate and the wing-stroke frequency (approximately 27 Hz), and changes in the position and accessibility of the metathoracic spiracle were visualized. The intersegmental cleft becomes constricted during downward bending of the wings by adduction of the metathorax to the mesothorax (Fig. 11B, Fig. 12A). Sp II becomes enclosed in the subalar cleft, and the external valve lip is probably pressed against the opposite soft intersegmental cuticle, closing the tracheal opening. In some individuals, a closing reflex of the spiracular lip could be induced by passive downward bending of the wings, and its wide reopening by wing lifting was clearly observed. During the upstroke and when the wing oscillates in the more upright position, as during shivering, the spiracle was visible with the external flap open (Fig. 11A,C, Fig. 12B).

Discussion

Unidirectional ventilatory air flow in the thorax

Hawkmoths are well known for their rapid and long-lasting flight. Regarded as among the most powerful flying insects, they are reminiscent of hummingbirds. The metabolic rate of *Manduca sexta* of 237 mW g^{-1} body mass (Casey, 1976) is similar to that of the hummingbird *Amazillia fimbriata* (232 mW g^{-1}; Berger and Hart, 1972). The present results go some way towards explaining the high O_2 content found in the active flight muscle (Komai, 1998), exceeding even the resting level in *Agrius convolvuli*. During steady flight, air is inspired through the anterior spiracles and expired through the posterior thoracic spiracles. Although the pressure maxima at the anterior spiracles are slightly positive (e.g. see Fig. 4), the negative mean pressure explains why CO_2 emission was not recorded from the anterior spiracles without further manipulation. The mean pressure difference between the anterior spiracles and the posterior air sacs (which are directly connected to the posterior thoracic spiracles) is obviously responsible for the unidirectional air flow. This air flow is so strong that an imposed pressure difference of more than 25 Pa was necessary to reverse it. Only under such an artificially increased counter-pressure in the posterior specimen chamber is CO_2 release at the anterior spiracles induced. Under these conditions, only intermittent flight occurred; the rate of CO_2 emission increased during the flight pauses by diffusion and decreased during flight phases (Fig. 9). This shows that the flight motor worked against the diffusive CO_2 outflow from the anterior spiracles even under this extreme artificial pressure difference; it was not possible to redirect all CO_2 emission through the anterior spiracles during flight. It cannot, as yet, be determined whether all the CO_2 measured was released from the posterior thoracic spiracles alone. Some CO_2 may also be

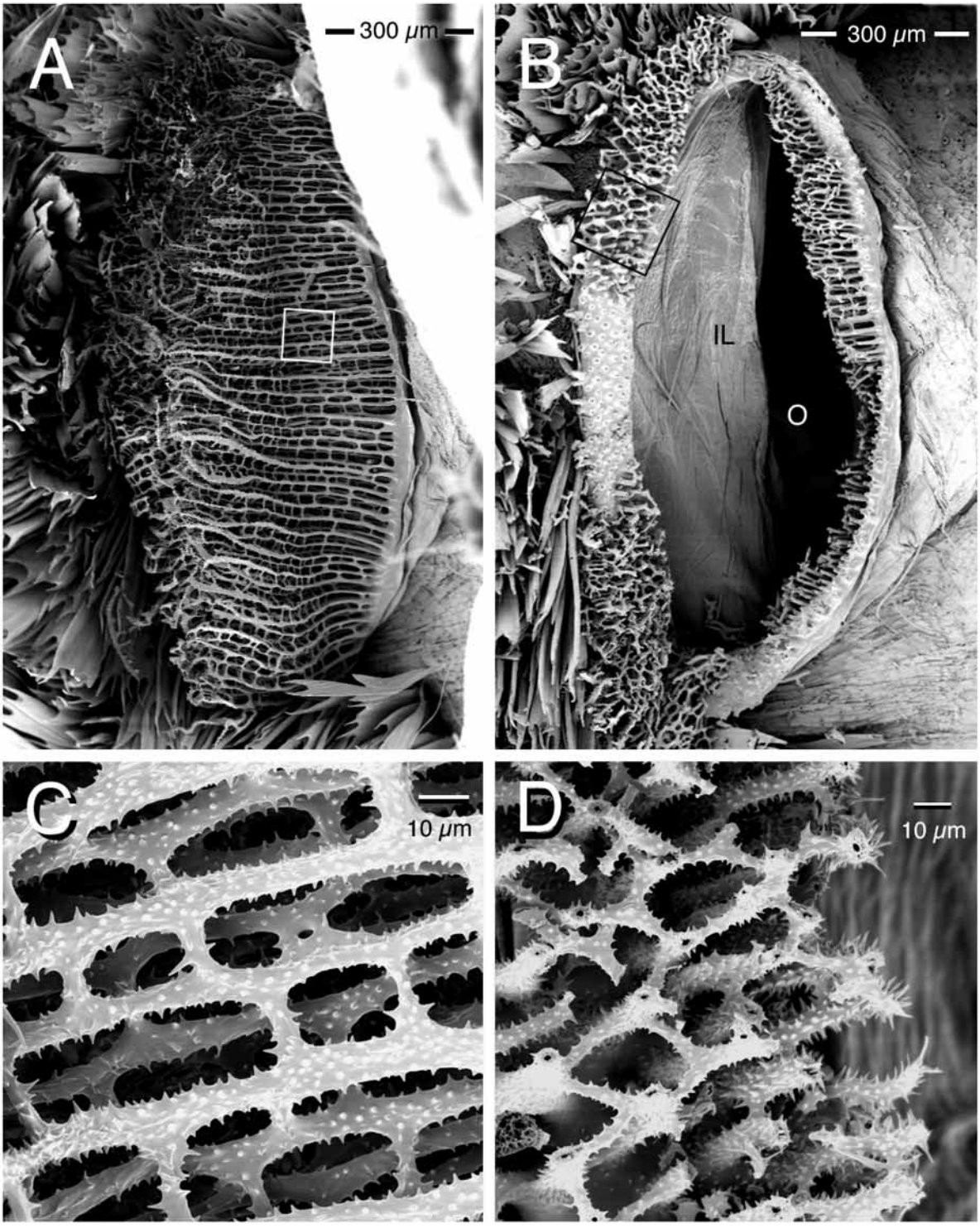

Fig. 10. Scanning electron micrographs of the anterior thoracic spiracle after descaling the prothoracic cuticle. (A) Peritrema with dense cuticular filter lamellae. (B) After removal of most of the filter lamellae, the half-opened inner valve lip (IL) and the orifice (O) are visible. (C) Outer layers of the filter meshwork; enlargement of boxed region in A. (D) Transverse section of the base of the anterior lamella revealing that approximately six rows of cuticle processes are connected by anastomoses. Enlargement of boxed region from B.

emitted from the first abdominal spiracles, which are connected to the thoracic tracheae. However, the first abdominal spiracles have an even denser peritrema filter structure than the anterior thoracic spiracles, suggesting that they might serve for inspiration rather than for expiration.

The unidirectional air stream observed in steady flight is not

operative during shivering, when the mean tracheal pressure at the anterior spiracles and the posterior air sac oscillates around atmospheric pressure and the amplitude of the pressure pulses at the anterior and the posterior spiracles was only one-third to one-quarter of the amplitude during steady flight (Fig. 3). During shivering, the mechanism is similar to autoventilation with a two-way (tidal) flow, as observed in *Schistocerca gregaria* (Miller, 1960; Weis-Fogh, 1967). In locusts, wing movements and the corresponding up and down movements of the nota result in air moving into and out of the anterior and posterior thoracic spiracles. In *Manduca sexta*, this flow becomes directional only with the greater downstroke amplitude that occurs during steady flight (Fig. 4, Fig. 5). At the anterior spiracles, as wingbeat amplitude increases, there is an increase in pressure amplitude correlated with a decrease in the mean pressure (Fig. 5A). At the mesoscutellar air sac, an increase in wingbeat amplitude is correlated with an increase in the mean pressure (Fig. 5B).

Komai (Komai, 1998) states that ‘a hawkmoth has no shunt mechanism in the primary tracheae’ and that ‘it does not use unidirectional ventilation flow and it is not known whether other large insects use unidirectional flow’. However, the experiments in which an artificially high pressure was imposed on the posterior spiracles from outside and induced emission of CO_2 through the anterior spiracles (Fig. 8, Fig. 9) provide further evidence for a unidirectional air flow. The minimum counter-pressure in the posterior chamber (ΔP) necessary for an air flow reversal to overcome the internal pressure gradient produced by the moth was approximately 25 Pa. This value corresponds to the lowest measured mean pressure gradient between the anterior spiracle and mesoscutellar air sac. This reversal of air flow must take place *via* longitudinal tracheae. Such a connection between the mesothoracic and metathoracic spiracles has been described in *Manduca sexta* (Eaton, 1988). Lateral primary tracheae with a simple spirally coiled intima could be traced from a complete histological series of transverse sections through the thorax and anterior abdomen of a smaller hawkmoth species *Proserpinus proserpina* (L. T. Wasserthal, unpublished data). These tracheal stems clearly connect the anterior spiracles with the air sacs of the mesothorax, the metathorax and the first abdominal segment and, thereby, the spiracles of these segments. Gas exchange during flight, under continuous mean negative pressure at the anterior spiracles, can only function with a corresponding mean positive pressure at the posterior spiracles.

Generation of unidirectional air flow by a thoracic suction pump

The intratracheal pressure maximum occurred at the end of the upstroke, and the haemocoel pressure measured in the locust was also greatest at this point (Weis-Fogh, 1967). This does not support the suggestion that the air sacs are compressed by contraction of the dorsal longitudinal muscles (DLMs) during the downstroke in *Agrius convolvuli* (Komai, 1998). According to the generally accepted model of indirect flight muscle systems (Pringle, 1975; Chapman, 1998), the thorax of hawkmoths is deformed by the action of the flight apparatus as follows. In *Manduca sexta*, wing upstroke is correlated with a slight flattening of the thorax caused by contraction of the dorsoventral muscles (DVMs), thus compressing the large air sacs lying between the tergites and the DLMs. These air sacs are continuous with the branching intramuscular air sacs (Fig. 2). During the downstroke, the thorax becomes slightly arched and shortened by contraction of the DLMs, increasing the volume of the posterior and dorsal thoracic air sacs. Thus, during the downstroke, the intratracheal pressure is negative (Fig. 6). During the downstroke, the posterior thoracic spiracles are covered by the intersegmental cleft and are probably closed by the valve flap fitting against the opposite cuticle, while the anterior spiracles remain open (Fig. 11B, Fig. 12), so air can be inspired unhindered only through the anterior spiracles and will be sucked posteriorly and dorsally into the large air sacs. Thus, a relatively simple mechanism involving volume changes of the thoracic air sacs together with the prevention of air inflow into the posterior thoracic spiracles is responsible for the retrograde air flow through the pterothorax. Whether the closing muscle of the posterior thoracic spiracle (Eaton, 1988; Nikam and Khole, 1989) is also involved in the closing mechanism during the downstroke needs to be investigated. Active closing and opening could be observed to result from passive wing bending in some individuals. It is probable that contraction of this closing muscle is synchronized with contraction of the DLMs, but a passive mechanism of valve closure may also be involved because the valve flap has no perforations and is unlikely to remain open against inspiratory suction, especially when the flap is close to the opposite cuticle. The role of the first abdominal spiracle, which communicates with the thoracic tracheal system, in the air supply mechanism is unclear. The first abdominal spiracles have an even denser peritrema filter structure than the anterior thoracic spiracles, so they are likely to serve for inspiration rather than for expiration.

The posterior thoracic spiracle as a valve for the expiratory air stream

The morphology of the posterior thoracic spiracle and its remarkable differences from the anterior spiracle have generated relatively little interest. The location of the posterior thoracic spiracle in the subalar cleft immediately below the wing hinge indicates that it is coupled to wing movements. In contrast to the extremely dense filter apparatus of the anterior spiracle (and of the first abdominal spiracle), the absence of any filter structures suggests that the posterior thoracic spiracle is adapted mainly for expiration. In contrast to all the other spiracles, it has no inner valve. It is only present after metamorphosis; caterpillars and pupae lack a functional spiracle on the metathoracic segment. The spinose margin of the valve lip and the spinose perispiracular cuticle could serve to prevent tight adhesion when the valve lip touches this soft cuticle.

Although the anterior spiracles are also open during the

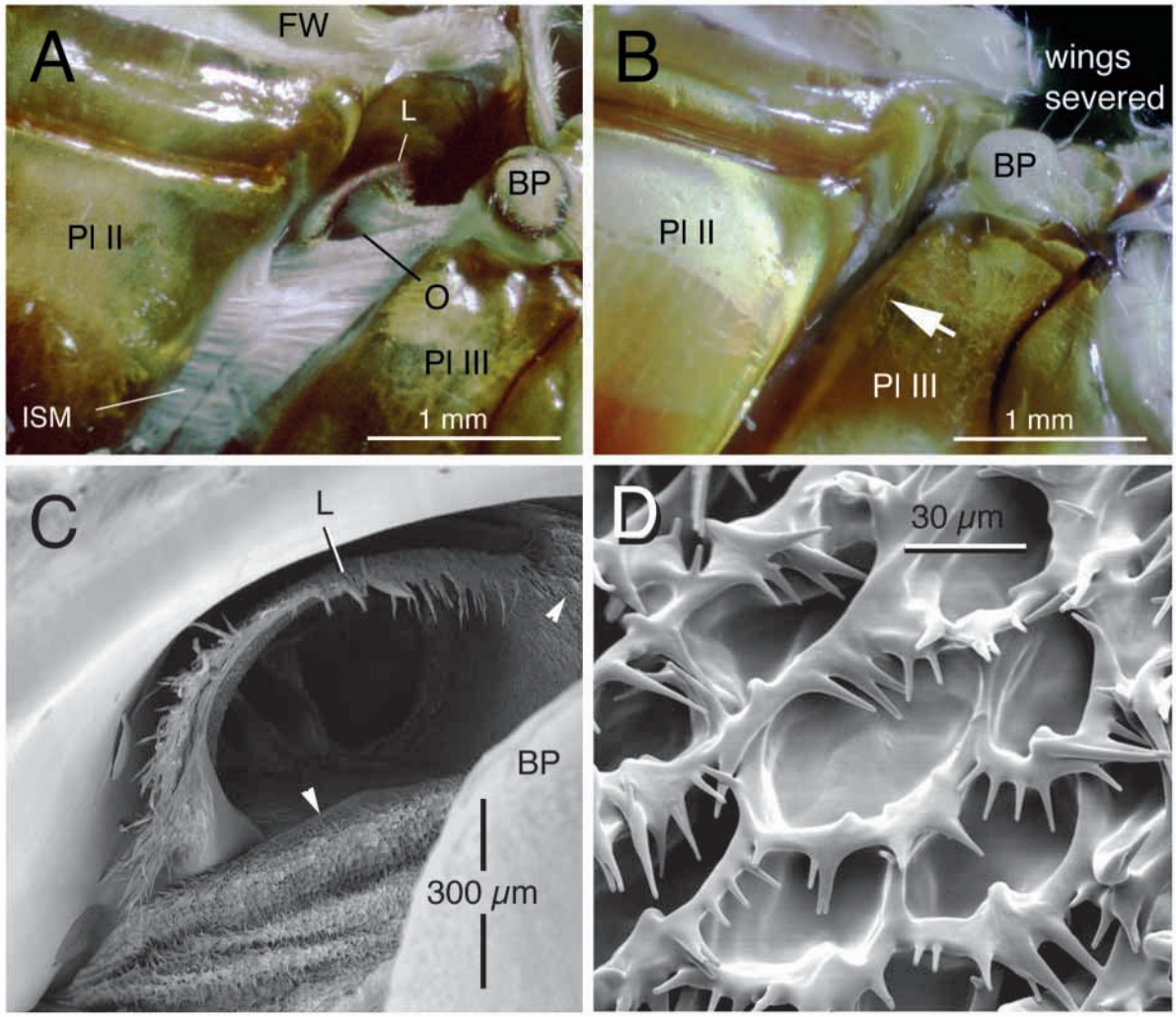

Fig. 11. Details of the posterior thoracic spiracle after descaling the cuticle around the wing hinge. (A,B) Light scanning micrographs. (A) Subalar intersegmental cleft with stretched intersegmental membrane (ISM) in extreme wing-up position showing the orifice (O) of the posterior spiracle with wide open external lip (L). (B) Intersegmental cleft constricted in the wing-down position enclosing the posterior spiracle. The metathorax is adducted to the mesothorax by contraction of the dorsal longitudinal muscles along the direction of the arrow. BP, basalar pad; FW, base of forewing; Pl II, pleuron of mesothorax; Pl III, pleuron of metathorax. (C,D) Scanning electron micrographs. (C) External valve lip (L) with marginal spines and spinose perispiracular cuticle (arrowheads). (D) Detail of cuticle at the transition between smooth tracheal intima and spinose perispiracular cuticle (see arrowheads in C).

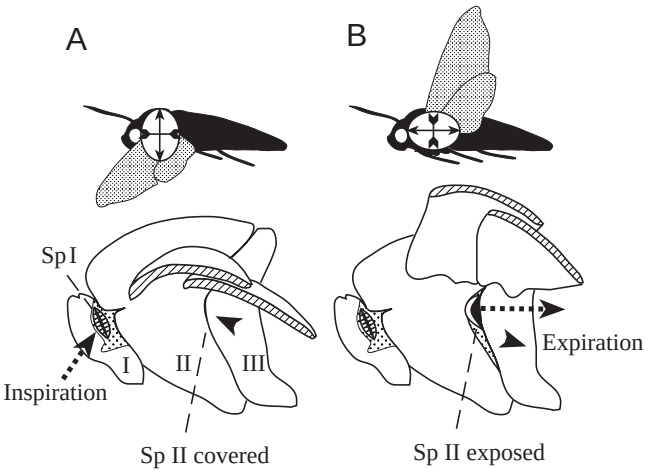

Fig. 12. Schematic lateral view of the thorax of *Manduca sexta* showing the deformation (arrows in upper diagrams) of the thorax during the downstroke (A) and upstroke (B) of the wings and its coupling with the adduction and retraction (arrowheads) of the metathorax enclosing and exposing the posterior thoracic spiracle (Sp II) in the subalar cleft. The increase in volume of the thoracic air sacs and closure of Sp II during the downstroke produce a retrogradely directed air stream, with inspiration through the anterior spiracles (Sp I) and expiration through the posterior thoracic spiracles (broken arrows). I, prothorax; II, mesothorax; III, metathorax.

upstroke, expiration through the posterior spiracles may be easier because of their vicinity to the large posterior air sacs and because of the absence of filter structures around Sp II, both of which should result in less resistance to the air stream.

Mechanisms of tracheal ventilation in flying insects

In other insect orders with similar fundamental differences between the anterior and posterior thoracic spiracles, a similar unidirectional air stream might occur during flight. While, in resting insects, observations of spiracular closing and opening behaviour have led to the conclusion that respiratory air flow is unidirectional during abdominal pumping movements (for references, see Mill, 1985), only few studies using split-chamber experiments have measured the effects of such directional air streams (Fraenkel, 1932b; Bailey, 1954; Wasserthal, 1996). For flying insects, three mechanisms of tracheal ventilation have been described: autoventilation with tidal flow, abdominal pumping and passive stream by the 'Fahrtwind'. The latter has been measured in cerambycid beetles and was termed the 'through-draught mechanism' (Miller, 1966). This retrograde air flow is suggested to be caused by the air stream passively entering the exposed anterior spiracles. A similar passive inflow of air into the anterior lepidopteran spiracles is unlikely because of the presence of dense scale layers and the peritrema filter apparatus. In flying locusts, a retrograde air stream produced by abdominal ventilatory movements is superimposed on the two-way autoventilation system (Miller, 1960; Weis-Fogh, 1967). In this case, all the thoracic spiracles are open during flight. The rate of flow through the spiracles is identical in both directions, so that no direction-sensitive valves are involved. The tidal flow of autoventilation mainly involves spiracles 2 and 3, while during abdominal pumping air is assumed to supply mainly the head *via* spiracles 1 (inspiration) and 5–10 (expiration) (Miller, 1960; Weis-Fogh, 1967). In *Schistocerca gregaria*, the haemolymph pressure amplitude near a ventral thoracic air sac was 100–150 Pa generated by the flight motor and 300–500 Pa generated by abdominal pumping (Weis Fogh, 1967). At 50–450 Pa, the pressure pulse amplitudes in *Manduca sexta* are within the range of values for the locust, but they are produced only by the the flight motor with no measurable contribution from abdominal pumping. Abdominal ventilatory movements have been described in other hawkmoth species (*Sphinx ligustri* and *Deilephila elpenor*) during flight (Fraenkel, 1932a). It is likely that the effects of these movements are restricted to the abdomen, as in the giant silk moth *Attacus atlas* at rest, where they are correlated with CO_2 bursts recorded from the abdominal chamber (Wasserthal, 1996).

Concluding remarks

The present results in *Manduca sexta* reveal a new mechanism for the supply of oxygen to the flight muscles and extend the spectrum of respiratory air supply mechanisms discussed above. The flight motor itself, by increasing thoracic volume during the downstroke and the simultaneous automatic closure of the metathoracic spiracle in the subalar cleft, produces a retrograde airflow through the pterothorax, with CO_2 output occurring only at the posterior spiracles. The flight-motor-driven retrograde air flow is reminiscent of a turbo engine that sucks fresh air in at the anterior openings and releases the used air through the posterior openings. This efficient respiratory air supply may provide part of the explanation for the increase in O_2 levels in sphingid flight muscles during steady flight (Komai, 1998) and the physiological basis for their powerful and long-lasting flight characteristics and hovering ability.

I thank Dr Joachim Schachtner, Marburg, for supplying us with eggs of *Manduca sexta* and Witold Lapinsky for rearing the animals. I am grateful to Thomas Messingschlager for constructing the apparatus and to Alfred Schmiedl for optimizing the electronic equipment. I am indebted to Dr Stefan Hetz for a helpful hint concerning pressure sensor calibration. Dr Wiltrud Wasserthal contributed by reading and discussing the manuscript. Her help and the stimulating recommendations of an anynomous referee and the text Editor Alison Cooper are gratefully acknowledged. The electronic equipment was partly financed by a grant of Deutsche Forschungs-Gemeinschaft (Wa 258/4-1, 4-2).

References

Bailey, L. (1954). The respiration currents in the tracheal system of the adult honey-bee. *J. Exp. Biol.* **31**, 589–593.

Bartholomew, G. A. and Casey, T. M. (1978). Oxygen consumption of moths during rest, pre-flight warm up and flight in relation to body size and wing morphology. *J. Exp. Biol.* **76**, 11–25.

Berger, M. and Hart, J. S. (1972). Die Atmung beim Kolibri *Amazillia fimbriata* während des Schwirrfluges bei verschiedenen Umgebungstemperaturen. *J. Comp. Physiol.* **81**, 363–380.

Casey, T. M. (1976). Flight energetics of sphinx moths: power input during hovering flight. *J. Exp. Biol.* **64**, 529–543.

Chapman, R. F. (1998). *The Insects.* Fourth edition. Cambridge: Cambridge University Press. 770pp.

Eaton, J. L. (1988). *Lepidopteran Anatomy*. Wiley-Interscience Series in Insect Morphology. New York: Wiley & Sons. 257pp.

Fraenkel, G. (1932a). Untersuchungen über die Koordination von Reflexen und automatisch-nervösen Rhythmen bei Insekten. II. Die nervöse Regulierung der Atmung während des Fluges. *Z. Vergl. Physiol.* **16**, 394–417.

Fraenkel, G. (1932b). Untersuchungen über die Koordination von Reflexen und automatisch-nervösen Rhythmen bei Insekten. III. Das Problem des gerichteten Atemstromes in den Tracheen der Insekten. *Z. Vergl. Physiol.* **16**, 418–443.

Gunlinson, S. L. and Harrison, J. F. (1997). Control of resting ventilation rate in grasshoppers. *J. Exp. Biol.* **199**, 379–389.

Hadley, N. F. (1994). Ventilatory patterns and respiratory transpiration in adult terrestrial insects. *Physiol. Zool.* **67**, 175–189.

Harrison, J. F. (1997). Ventilatory mechanisms and control in grasshoppers. *Am. Zool.* **37**, 73–81.

Hetz, S. K., Psota, E. and Wasserthal, L. T. (1999). Roles of aorta, ostia and tracheae in heartbeat and respiratory gas exchange in pupae of *Troides rhadamantus* Staudinger 1888 (Ornithoptera, Papilionidae). *Int. J. Insect Morph.* **28**, 131–144.

Hetz, S. K., Wasserthal, L. T., Hermann, S., Kaden, H. and Oelßner, W. (1993). Direct oxygen measurements in the tracheal system of lepidopterous pupae using miniaturized amperometric sensors. *Bioelectrochem. Bioenerg.* **33**, 165–170.

Kestler, K. (1984). Respiration and respiratory water loss. In *Environmental Physiology and Biochemistry of Insects* (ed. K. H. Hoffmann), pp. 247–280. Berlin, Heidelberg: Springer

Komai, Y. (1998). Augmented respiration in a flying insect. *J. Exp. Biol.* **201**, 2359–2366.
Lighton, J. R. B. (1996). Discontinuous gas exchange in insects. *Annu. Rev. Ent.* **141**, 309–324.
Mill, P. J. (1985). Structure and physiology of the respiratory system. *Comp. Insect Physiol. Biochem. Pharmac.* **3**, 517–593.
Miller, P. L. (1960). Respiration in the desert locust. III. Ventilation and the spiracles during flight. *J. Exp. Biol.* **37**, 264–278.
Miller, P. L. (1966). The supply of oxygen to the active flight muscles of some large beetles. *J. Exp. Biol.* **45**, 285–304.
Miller, P. L. (1974). Respiration – aerial gas transport. In *The Physiology of Insecta*, vol. 6 (ed. M. Rockstein), pp. 345–402. New York: Academic Press.
Miller, P. L. (1981). Ventilation in active and inactive insects. In *Locomotion and Energetics in Arthropods* (ed. C. F. Herreid and C. R. Fourtner), pp. 317–390. New York: Plenum Press.
Nikam, T. B. and Khole, V. V. (1989). *Insect Spiracular Systems.* Chichester: Ellis Horwood Ltd. 136pp.
Nüesch, H. (1953). The morphology of the thorax of *Telea polyphemus* (Lepidoptera). I. Skeleton and muscles. *J. Morph.* **93**, 589–609.
Pringle, J. W. S. (1975). Insect flight. *Oxford Biol. Readers* **52**, 1–16.
Slama, K. (1976). Insect haemolymph pressure and its determination. *Acta Ent. Bohemoslov.* **73**, 65–75.
Slama, K. (1988). A new look at insect respiration. *Biol. Bull.* **175**, 289–300.
Snodgrass, R. E. (1935). *Principles of Insect Morphology*. New York: McGraw-Hill. 667pp.
Wasserthal, L. T. (1976). Heartbeat reversal and its coordination with accessory pulsatile organs and abdominal movements in Lepidoptera. *Experientia* **32**, 577–578.
Wasserthal, L. T. (1981). Oscillating haemolymph 'circulation' and discontinuous tracheal ventilation in the giant silk moth *Attacus atlas* L. *J. Comp. Physiol.* **145**, 1–15.
Wasserthal, L. T. (1982). Antagonism between haemolymph transport and tracheal ventilation in an insect (*Attacus atlas* L.). *J. Comp. Physiol.* **147**, 27–40.
Wasserthal, L. T. (1996). Interaction of circulation and tracheal ventilation in holometabolous insects. *Adv. Insect Physiol.* **26**, 297–351.
Wasserthal, L. T. (1999). Functional morphology of the heart and of a new cephalic pulsatile organ in the blowfly *Calliphora vicina* (Dipt.: Calliphoridae) and their roles in hemolymph transport and tracheal ventilation. *Int. J. Insect Morph. Embryol.* **28**, 111–129.
Weis-Fogh, T. (1964a). Functional design of the tracheal system of flying insects as compared with the avian lung. *J. Exp. Biol.* **41**, 207–227.
Weis-Fogh, T. (1964b). Diffusion in insect wing muscle, the most active tissue known. *J. Exp. Biol.* **41**, 229–256.
Weis-Fogh, T. (1967). Respiration and tracheal ventilation in locusts and other flying insects. *J. Exp. Biol.* **47**, 561–587.